TD-DFT study of the absorption and emission spectra of blue to red phosphorescent Ir(III) complexes

TUGBA TUGSUZ

Department of Chemistry, Hacettepe University, Beytepe, Ankara 06800, Turkey

The electronic structures and spectroscopic properties of a series of blue to red emitted tris-chelated Ir(III) complexes containing two cyclometalating ligands (2-(4,6-difluorophenyl)-4-methoxypyridine (LB), 4,4'-difluoro-5-methyl-2,3-diphenylpyrazine (LG), 5-methyl-2,3-diphenylpyrazine (LY), 2,3-bis(4-fluorophenyl)-quinoxaline (LO), 2,3-diphenylquinoxaline (LR)) and one ancillary ligand (acetylacetonate (acac)) were investigated at the B3LYP/6-31G(d)+LANL2DZ, B3LYP/TZVP, PBE0/6-31G(d)+LANL2DZ and PBE0/TZVP levels. Time-dependent density functional theory (TD-DFT) method with PCM model in CH_2Cl_2 solution was employed to explore the absorption and emission properties based on the optimized geometries in the ground state. The lowest lying absorptions of complexes were calculated to be of triplet character, essentially corresponding to HOMO→LUMO and HOMO→LUMO+1 transitions with metal-to-ligand charge transfer (^{3}MLCT) transitions. The phosphorescence of each complex originates from the lowest triplet excited state, which is assigned to the mixing of ^{3}MLCT and intraligand charge transfer characters. Finally we found extremely good agreement between theory and experiment, thus we suggest that the computational analysis applied here can open the way to a theoretical and computational strategy for the design and preparation of new red to blue colored phosphorescent iridium compounds.

1. Introduction

Phosphorescent organic materials have attracted much attention due to their potential use in various optoelectronic applications, in material design and recently in device fabrication [1]. Although phosphorescence, in principle originated from the spin-forbidden triplet state, it can be achieved through the spin-orbit coupling, leading to mixing of the singlet and triplet excited states of heavy metals. Among these heavy metals, Ir(III) is the most effective and its tris-chelated complexes are known to have high internal efficiency and high phosphorescence [2]. A tris-chelated neutral Ir(III) complex consists of a core Ir atom and three anionic ligands. If all ligands are identical, complexes are homoleptic, otherwise they are heteroleptic. Usually, heteroleptic Ir(III) complexes comprise two cyclometalating ligands (C^N) and one ancillary ligand [1,3,4,5]. In this work we studied the blue to red colored phosphorescent heteroleptic tris-chelated Ir(III) complexes.
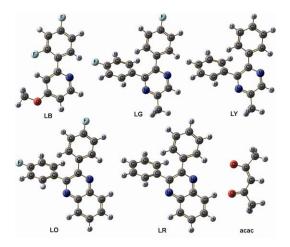
On the basis of geometry optimization of structures, the B3LYP [6] functional appears to be the best choice for molecules containing first and second row atoms [7]. However, for systems containing transition metal atoms the selection of functional is not so obvious.

More recently, regarding molecular geometries and simple reactions, it is found that Becke's generalized gradient approximation (GGA) exchange functional in 1988 [8] together with Perdew's 1986 correlation part (BP86) [9] gives better results for geometries of transition metal complexes [10]. Di Censo et al. [5] has also used BP86 exchange correlation functional for their iridium complexes and they have found good correlation in their optimized geometry results with X-ray data of their similar analog of complexes. In this work in order to optimize the tris-chelated Ir(III) complexes, we have also chosen the BP86 functional, because of better accuracy in the geometries of transition metal complexes.

The possibility to predict the electronic properties, especially the excited states of transition metal compounds by using theoretical calculations, is of great importance. The time dependent density functional theory, TD-DFT [11] has been successfully applied on the excited states of the transition metal complexes, regardless of their spin and symmetry [12]. TD-DFT computational procedure allows us to provide a detailed assignment of the excited states involved in the absorption and emission processes. TD-DFT calculations of electronic transitions are based on the response of the ground-state electron density to the oscillating optical field. The use of the ground-state density makes the question of the validity of the Hohenberg-Kohn theorems to excited states irrelevant [13].

In this work we present extensive DFT and TD-DFT investigations concerning the structures and spectroscopic properties of blue to red emitted phosphorescent tris-chelated Ir(III) complexes by using two cyclometalating ligands, namely 2-(4,6-difluorophenyl)-4-methoxypyridine (LB), 4,4'-difluoro-5-methyl-2,3-diphenylpyrazine (LG), 5-methyl-2,3-diphenylpyrazine (LY), 2,3-bis(4-fluorophenyl)-quinoxaline (LO), 2,3-

diphenylquinoxaline (LR) and acetylacetonate (acac) ancillary ligand (Scheme I).

The ground state (S_0) and (T_1) of Ir(LB)$_2$(acac), Ir(LG)$_2$(acac), Ir(LY)$_2$(acac), Ir(LO)$_2$(acac) and Ir(LR)$_2$(acac) (where LB, LG, LY, LO and LR representing the ligands of blue, green, yellow, orange and red, respectively) complex geometries, were calculated by adopting the BP86 exchange correlation functional while for the low-lying triplet and singlet excited states TD-DFT calculations were used.

Scheme 1. The cyclometalating ligands (2-(4,6-difluorophenyl)-4-methoxypyridine (LB), 4,4'-difluoro-5-methyl-2,3-diphenylpyrazine (LG), 5-methyl-2,3-diphenylpyrazine (LY), 2,3-bis(4-fluorophenyl)-quinoxaline (LO), 2,3-diphenylquinoxaline (LR) and ancillary ligand acetylacetonate (acac).

2. Computational details

The geometries of Ir(LB)$_2$(acac), Ir(LG)$_2$(acac), Ir(LY)$_2$(acac), Ir(LO)$_2$(acac) and Ir(LR)$_2$(acac) complexes were optimized using the BP86 exchange-correlation functional of DFT [8,9] together with triple ζ" quality and polarization basis set, TZVP [14] for C, H, N, O and F

atoms and def-TZVP basis set for Ir atom in the TURBOMOLE 6.3 program [15]. Geometry optimizations were performed imposing C$_2$ symmetry for both the singlet ground state (S_0) and triplet state (T_1). Molecular orbital energies of ground state structures were derived from B3LYP [6] and PBE0 [16] hybrid functionals together with TZVP and 6-31G(d) basis sets for C, H, N, O and F atoms and LANL2TZ(f) [17,18] and LANL2DZ [17,19] basis sets for the Ir atom in dichloromethane (CH$_2$Cl$_2$) solution by means of the Polarizable Continuum Model, PCM [20] as implemented in the Gaussian 09 program package [21]. The cavity for solute molecule was built from a group of overlapping spheres. The universal force field (UFF) model which places a sphere around each solute atom was applied to build up the molecular cavity. On the basis of optimized geometries, TD-DFT calculations for spectroscopic properties were performed by Gaussian 09 program package. The lowest 50 singlet-singlet and 10 singlet-triplet excitations in CH$_2$Cl$_2$ solution have been computed by means of TD-DFT for all complexes at both the ground state singlet S_0 and lowest excited triplet state T_1 optimized geometries.

3. Results and discussion

3.1. Geometry and electronic structure

The singlet ground state (S_0) molecular structures of Ir(LB)$_2$(acac), Ir(LG)$_2$(acac), Ir(LY)$_2$(acac), Ir(LO)$_2$(acac) and Ir(LR)$_2$(acac) complexes in C$_2$ symmetry were optimized at BP86/TZVP level. The selected geometrical parameters of all complexes are summarized in Table 1 and the optimized geometries are shown in Fig. 1. Because of C$_2$ symmetry, the two LB, LG, LY, LO and LR ligands were found almost perpendicular to each other in all complexes. The calculated Ir-C, Ir-N and Ir-O distances are in good agreement with the experimental X-ray data range [22].

Table 1. Main optimized geometrical parameters of the Ir(LB)$_2$(acac), Ir(LG)$_2$(acac), Ir(LY)$_2$(acac), Ir(LO)$_2$(acac) and Ir(LR)$_2$(acac) complexes in the ground state at the BP86/TZVP level together with the experimental values.

	Ir(LB)$_2$(acac)	Ir(LG)$_2$(acac)	Ir(LY)$_2$(acac)	Ir(LO)$_2$(acac)	Ir(LR)$_2$(acac)	Expt. [a]
Bond lengths (Å)						
Ir-N1	2.066	2.053	2.051	2.085	2.083	2.043(5)
Ir-C1	2.008	2.009	2.010	1.999	2.000	1.976(6)
Ir-O1	2.203	2.210	2.218	2.222	2.229	2.136(4)
Bond angles (°)						
∠N1-Ir-N2	177.4	178.0	178.6	178.3	178.4	176.3(4)
∠C1-Ir-C2	92.54	92.73	92.71	93.70	94.03	
∠O1-Ir-O2	86.87	86.83	86.49	85.49	85.15	90.0(3)
∠N1-Ir-C1	80.22	79.97	79.88	79.58	79.53	81.7(4)
∠N1-Ir-O2	94.72	94.16	94.16	99.49	99.48	94.5(3)
∠C1-Ir-O1	90.50	90.50	90.68	90.41	90.41	87.5(3)
Dihedral angle (°)						
∠C3-N2-Ir-C1	96.87	103.9	105.2	113.0	113.6	

a) Laskar et al., Lamansky et al. [15-17]

The Ir-N bond lengths are 0.058, 0.044, 0.041, 0.086 and 0.083 Å longer than the Ir-C bond lengths in Ir(LB)$_2$(acac), Ir(LG)$_2$(acac), Ir(LY)$_2$(acac), Ir(LO)$_2$(acac) and Ir(LR)$_2$(acac) complexes, respectively. The Ir(LO)$_2$(acac) and Ir(LR)$_2$(acac) complexes have the biggest bond length differences which can be attributed to the steric hindrance effect of the quinoxaline ligand.

3.2. Molecular Orbitals in Ground States:

Due to their structural similarity, the frontier orbitals of green and yellow complexes (Ir(LG)$_2$(acac) and Ir(LY)$_2$(acac)) have shown similar compositions. The same result was also found for the orange and red complexes (Ir(LO)$_2$(acac) and Ir(LR)$_2$(acac)). The frontier molecular orbitals of blue (Ir(LB)$_2$(acac)), green-yellow and orange-red emitted iridium complexes in their ground states are depicted in Fig. 2, Fig. 3 and Fig. 4, and the descriptions of frontier molecular orbital energies and compositions are summarized in Table 2, Table 3 and Table 4, respectively. Because of the similarity in shapes and contributions of the frontier orbitals of green-yellow and orange-red, the orbitals of only green and orange colored iridium complexes are depicted in Figure 3 and Figure 4, respectively. All DFT calculations indicated that the lowest unoccupied molecular orbital (LUMO) had contribution from the LB, LG, LY, LO, LR parts of ligand and no significant interaction between the ligand and the metal-centered orbitals can be observed in the LUMOs. The calculated LUMO of the blue to red complexes are at -1.416, -2.036, -1.971, -2.561 and -2.496 eV, respectively. The LUMO of the blue complex is mainly composed of a p orbital of C, while green to red complexes have p orbital composition of N in their LUMO. The computed HOMO of all complexes has a strong overlap with the d orbital of Ir atom. The contribution of d orbitals of the Ir atom to the HOMO, ranges from 34% to 46.8%. The computed energies of HOMO level of the blue to red complexes showed a relatively small change (~0.2 eV) as -5.723, -5.736, -5.552, -5.829 and -5.640 eV, respectively. The H-1 of all blue to red complexes is composed of d orbitals of the Ir atom and p orbital of the C and O atoms of the ancillary acac ligand. The H-2 level of blue and H-3 level of green to red complexes have mainly d orbital contribution of Ir, while the H-3 level of blue and H-2 levels of green to red complexes have p orbitals of C at the LB, LG, LY, LO, LR ligand moiety.
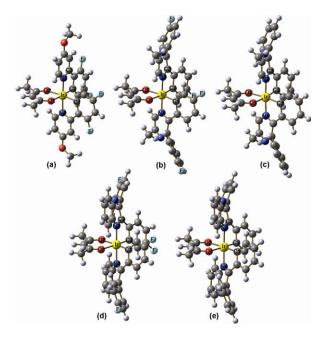

Fig. 1. The singlet ground state (S$_0$) molecular structure of a) Ir(LB)$_2$(acac), b) Ir(LG)$_2$(acac), c) Ir(LY)$_2$(acac), d) Ir(LO)$_2$(acac) and e) Ir(LR)$_2$(acac) complexes.

Table 2. Molecular orbital energies and compositions of Ir(LB)$_2$(acac) in the ground state at the PBE0/6-31G(d)+LANL2DZ.

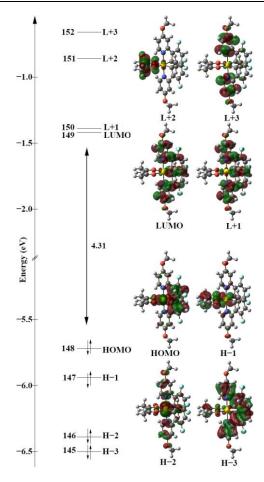| Ir(LB)$_2$(acac)	Orbital	Energy(eV)	MO composition
L+6	155	0.271	C p=0.46
L+5	154	0.081	C p=0.48
L+4	153	-0.596	C p=0.58
L+3	152	-0.663	C p=0.32
L+2	151		C p=0.62
		-0.863	O p=0.24
L+1	150	-1.388	C p=0.22
LUMO	149	-1.416	C p=0.20
HOMO	148	-5,723	Ir d=0.44
H-1	147		Ir d=0.36
			C p=0.25
		-5,935	O p=0.22
H-2	146	-6,390	Ir d=0.54
H-3	145	-6,503	C p=0.09
H-4	144	-6,695	Ir d=0.12
H-5	143		Ir d=0.18
		-6,716	C p=0.17
H-6	142	-6,984	C p=0.28

Fig. 2. The frontier molecular orbitals of Ir(LB)₂(acac) complex.

Table 3. Molecular orbital energies and compositions of Ir(LG)₂(acac) and Ir(LY)₂(acac) in the ground state at the PBE0/6-31G(d)+LANL2DZ.

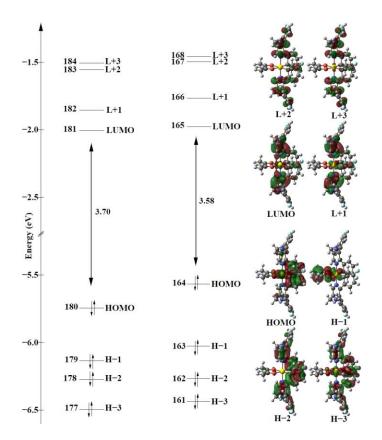|		Ir(LO)₂(acac)			Ir(LR)₂(acac)	
	Orbital	Energy(eV)	MO composition	Orbital	Energy(eV)	MO composition
L+6	205	-0,444	C p=0.86	189	-0,148	C p=0.64
L+5	204	-0,502	C p=0.20	188	-0,209	C p=0.20
L+4	203		C p=0.62	187		C p=0.62
		-0,969	O p=0.24		-0,887	O p=0.24
L+3	202	-1,545	C p=0.08	186	-1,490	C p=0.09
L+2	201	-1,550	C p=0.09	185	-1,491	C p=0.08
L+1	200	-2,339	N p=0.09	184	-2,263	N p=0.09
LUMO	199	-2,561	N p=0.09	183	-2,496	N p=0.09
HOMO	198	-5,829	Ir d=0.34	182	-5,640	Ir d=0.37
H-1	197		Ir d=0.22	181		Ir d=0.24
			C p=0.31			C p=0.30
		-6,112	O p=0.28		-6,011	O p=0.26
H-2	196	-6,339	C p=0.07	180	-6,336	C p=0.07
H-3	195	-6,559	Ir d=0.10	179	-6,504	Ir d=0.08
H-4	194			178		Ir d=0.11
		-6,719	C p=0.11		-6,638	C p=0.14
H-5	193	-6,773	Ir d=0.24	177	-6,687	Ir d=0.33
H-6	192	-7,025	C p=0.10	176	-6,801	C p=0.08

Fig. 3. The frontier molecular orbitals of green-yellow (Ir(LG)₂(acac)-Ir(LY)₂(acac)) complexe

Table 4. Molecular orbital energies and compositions of Ir(LO)₂(acac) and Ir(LR)₂(acac)
in the ground state at the PBE0/6-31G(d)+LANL2DZ

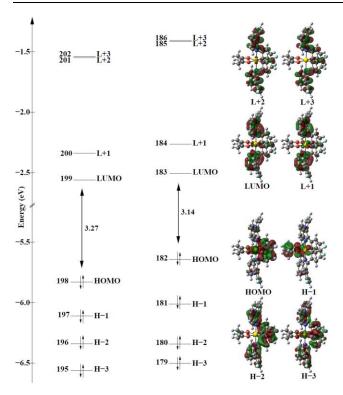|		Ir(LG)₂(acac)			Ir(LY)₂(acac)	
	Orbital	Energy(eV)	MO composition	Orbital	Energy(eV)	MO composition
L+6	187	-0.416	C p=0.92	171	-0,111	C p=0.90
L+5	186	-0.458	C p=0.44	170	-0,161	C p=0.44
L+4	185	-0.959	C p=0.62 O p=0.24	169	-0,876	C p=0.62 O p=0.24
L+3	184	-1.504	C p=0.22	168	-1,449	C p=0.22
L+2	183	-1.549	C p=0.20	167	-1,494	C p=0.22
L+1	182	-1.849	N p=0.22	166	-1,759	N p=0.22
LUMO	181	-2.036	N p=0.22	165	-1,971	N p=0.22
HOMO	180	-5,736	Ir d=0.36	164	-5,552	Ir d=0.39
H-1	179	-6,128	Ir d=0.25 C p=0.32 O p=0.28	163	-6,024	Ir d=0.27 C p=0.31 O p=0.26
H-2	178	-6,271	C p=0.08	162	-6,262	C p=0.08
H-3	177	-6,491	Ir d=0.12	161	-6,426	Ir d=0.10
H-4	176	-6,854	Ir d=0.70	160	-6,665	C p=0.10
H-5	175	-6,906	Ir d=0.20 C p=0.12	159	-6,699	Ir d=0.67
H-6	174	-7,105	Ir d=0.08	158	-6,960	Ir d=0.22

Fig. 4. The frontier molecular orbitals of orange-red (Ir(LO)$_2$(acac)-Ir(LR)$_2$(acac)) complexes.

3.3. Absorption spectra of Ir(III) complexes

The absorption spectra of blue to red colored iridium complexes have been widely studied experimentally [22,26]. Here, we present detailed TD-DFT analysis of these complexes obtained from the B3LYP and PBE0 functionals which are the most popular methods due to their good agreement with experimental data [3,5,27]. We selected triple (TZVP+defTZVP) and double zeta (6-31G(d)+LANL2DZ) properties of basis sets for detailed calculations. The selected absorption bands of the Ir(LB)$_2$(acac), Ir(LG)$_2$(acac), Ir(LY)$_2$(acac), Ir(LO)$_2$(acac) and Ir(LR)$_2$(acac) complexes in the UV–Vis region simulated in CH$_2$Cl$_2$ solution associated with their main configurations and the assignments as well as the experimental results, are given in Table 5. The absorption spectra of the investigated complexes in all computations showed similar configurations either with the MLCT, LLCT characters or with both of them. The absorption bands of the complexes in the region between 276 and 414 nm can be assigned to the spin-allowed singlet metal-to-ligand charge transfer (^{1}MLCT), while those observed in the region between 433 and 672 nm are assignable to the spin-forbidden triplet ^{3}MLCT, which have zero oscillator strengths, because of spin–orbit coupling in the TDDFT calculations. The highest energy and the lowest absorption bands of complexes, except those from Ir(LY)$_2$(acac), were calculated to quite an intense ^{1}MLCT character. For Ir(LY)$_2$(acac), the highest energy band was calculated at LLCT character. The other higher energy bands of complexes were calculated as having MLCT, LLCT and both MLCT and LLCT characters. The lowest energy bands of complexes were found to be of triplet character essentially corresponding to HOMO→LUMO and HOMO→LUMO+1 ^{3}MLCT transitions.

We were indeed able to reproduce the nature of the main spectral features and their relative intensities by using different computational methods. The experimental results of (LB)$_2$(acac), Ir(LG)$_2$(acac), Ir(LY)$_2$(acac), Ir(LO)$_2$(acac) and Ir(LR)$_2$(acac) complexes have the lowest-lying absorptions at 383, 275, 335, 378 and 285 nm, respectively. The closest bands to the experimental lowest absorption measurements were calculated for Ir(LB)$_2$(acac) at 391, 372, 374 and 388 nm, for Ir(LG)$_2$(acac) at 286, 297, 276 and 284 nm, for Ir(LY)$_2$(acac) at 312, 317, 348 and 353 nm, for Ir(LO)$_2$(acac) at 383, 379, 367 and 370 nm, for Ir(LR)$_2$(acac) at 293, 299, 284 and 287 nm by using B3LYP/6-31G(d)+LANL2DZ, B3LYP/TZVP+def-TZVP, PBE0/6-31G(d)+LANL2DZ and PBE0/TZVP+def-TZVP methods, respectively. Moreover, the computed absorption bands at 343, 331, 314 and 316 nm for Ir(LG)$_2$(acac), at 364, 369, 379 and 391 nm for Ir(LY)$_2$(acac), at 393, 396, 381 and 382 nm for Ir(LO)$_2$(acac), at 379, 396, 376 and 380 nm for Ir(LR)$_2$(acac) agree reasonably well with experimental 386, 388, and 378 nm values, respectively. The calculated triplet excited states of complexes provided by TD-DFT calculations from their ground state geometry essentially correspond to HOMO→LUMO and HOMO→LUMO+1 ^{3}MLCT transitions. Thus spin-forbidden singlet-triplet transitions become allowed due to the strong spin-orbit coupling of the Ir(III) center. The experimental lowest singlet-triplet transitions of (LB)$_2$(acac), Ir(LG)$_2$(acac), Ir(LY)$_2$(acac), Ir(LO)$_2$(acac) and Ir(LR)$_2$(acac) complexes are located at 419, 530, 507, 543 and 625 nm, respectively. The absorption maxima of (LB)$_2$(acac), Ir(LY)$_2$(acac), Ir(LO)$_2$(acac) and Ir(LR)$_2$(acac) complexes computed from B3LYP/6-31G(d)+LANL2DZ and PBE0/6-31G(d)+LANL2DZ methods are in good agreement with experimental data with 14 and 16 nm, 18 and 15 nm, 51 and 57 nm, 18 and 17 nm differences, respectively. For the Ir(LG)2(acac) complex all computational methods gave results closer to the experimental maximum absorption measurement.

Table 5. Calculated lowest transitions in nm, oscillator strengths f>0.02)[b] related to the experimental absorption spectra for Ir(LB)₂(acac), Ir(LG)₂(acac), Ir(LY)₂(acac), Ir(LO)₂(acac) and Ir(LR)₂(acac)

	B3LYP/ 6-31G(d) +LANL2DZ	Δλ	B3LYP/ TZVP +def-TZVP	Δλ	PBE0/ 6-31G(d) +LANL2DZ	Δλ	PBE0/ TZVP +def-TZVP	Δλ	Dominant transitions and assignments	Expt.
Ir(LB)₂(acac)	326 (3.80)	57	343 (3.62)	40	313 (3.96)	70	327 (3.79)	56	H-2→L (MLCT)	383
	360 (3.44)	23	372 (3.33)	11	344 (3.60)	39	354 (3.50)	29	H-1→L+1 (MLCT-LLCT)	
	391 (3.17)	8	407 (3.05)	24	374 (3.32)	9	388 (3.20)	5	H→L (MLCT)	
	433 (2.86)	14	445 (2.79)	26	435 (2.85)	16	445 (2.79)	26	H→L+1 (³MLCT)	
	438 (2.83)	19	450 (2.76)	31	439 (2.82)	20	449 (2.76)	30	H→L (³MLCT)	419
Ir(LG)₂(acac)	286 (4.34)	11	297 (4.18)	22	276 (4.49)	1	284 (4.37)	9	H→L+5 (MLCT)	275
	316 (3.92)	14	319 (3.89)	11	304 (4.08)	26	307 (4.04)	23	H-2→L+3 (LLCT)	
	343 (3.62)	13	331 (3.75)	1	314 (3.95)	26	316 (3.92)	14	H-3→L+1 (MLCT)	330
	367 (3.38)	13	370 (3.35)	10	351 (3.53)	29	354 (3.50)	26	H-2→L (LLCT)	380
	385 (3.22)	5	398 (3.12)	18	365 (3.40)	15	376 (3.30)	4	H→L+2 (MLCT)	
	410 (3.02)	15	417 (2.97)	8	390 (3.18)	35	397 (3.12)	28	H-1→L (MLCT-LLCT)	425
	514 (2.41)	16	523 (2.37)	7	514 (2.41)	16	522 (2.38)	8	H→L+1 (MLCT)	
	529 (2.34)	1	544 (2.28)	14	522 (2.38)	8	533 (2.33)	3	H→L (MLCT)	530
Ir(LY)₂(acac)	312 (3.97)	23	317 (3.91)	18	303 (4.09)	32	307 (4.04)	28	H-2→L+3 (LLCT)	335
	364 (3.41)	29	369 (3.36)	34	348 (3.56)	13	353 (3.51)	18	H-2→L (LLCT)	
	400 (3.10)	14	414 (3.00)	28	379 (3.27)	7	391 (3.17)	5	H→L+2 (MLCT)	386
	416 (2.98)	30	424 (2.92)	38	396 (3.13)	10	404 (3.07)	18	H-1→L (MLCT-LLCT)	
	525 (2.36)	18	537 (2.31)	30	522 (2.38)	15	531 (2.33)	24	H→L+1 (MLCT)	
	549 (2.26)	42	567 (2.19)	60	536 (2.31)	29	551 (2.25)	44	H→L (MLCT)	507
Ir(LO)₂(acac)	383 (3.24)[b]	5	379 (3.27)[c]	1	367 (3.38)[b]	11	370 (3.35)[b]	8	b)H-4→L (LLCT)	378
	393 (3.16)[d]	5	396 (3.13)[e]	8	381 (3.25)[e]	7	382 (3.25)[d]	6	c)H-5→L d)H-2→L+1 (LLCT)	388
	416 (2.98)	28	417 (2.97)	29	397 (3.12)	9	399 (3.11)	11	e)H-3→L H-2→L (LLCT)	
	482 (2.57)	17	487 (2.55)	22	459 (2.70)	6	464 (2.67)	1	H-1→L (MLCT-LLCT)	465

	B3LYP/6-31G(d)+LANL2DZ	Δλ	B3LYP/TZVP+def-TZVP	Δλ	PBE0/6-31G(d)+LANL2DZ	Δλ	PBE0/TZVP+def-TZVP	Δλ	Dominant transitions and assignments	Expt.
	594 (2.09)	51	603 (2.06)	60	600 (2.07)	57	608 (2.04)	65	H→L+1 (MLCT)	
	620 (2.00)	77	637 (1.95)	94	612 (2.03)	69	624 (1.99)	81	H→L (MLCT)	543
Ir(LR)$_2$(acac)	293 (4.23)[f]	8	299 (4.15)[f]	14	284 (4.37)[g]	1	287 (4.32)[g]	2	f)H-4→L+2 g)H-3→L+2 (MLCT)	285
	379 (3.27)[h]	1	396 (3.13)[h]	18	376 (3.30)[i]	2	380 (3.26)[i]	2	h)H-3→L+1 (MLCT)	378
	410 (3.02)	32	414 (3.00)	36	392 (3.16)	14	395 (3.14)	17	i)H-3→L H-2→L (LLCT)	
	490 (2.53)		496 (2.50)		467 (2.66)		472 (2.63)		H-1→L (MLCT-LLCT)	476
	607 (2.04)	18	621 (2.00)	4	608 (2.04)	17	619 (2.00)	6	H→L+1 (MLCT)	
	649 (1.91)	24	672 (1.85)	47	632 (1.96)	7	650 (1.91)	25	H→L (MLCT)	625

b) For singlet-triplet transitions, oscillator strengths are zero because of the neglect of spin-orbit coupling in the TD-DFT calculations.

3.4. Emission spectra of Ir(III) complexes:

To gain insight into the emission process of the blue to red colored phosphorescence iridium complexes, we analyzed the 10 lowest singlet-triplet excitations calculated at the lowest excited triplet state T_1 optimized geometries. The calculated phosphorescence emission energies and characters of all complexes in CH_2Cl_2 solution together with the corresponding experimental values [22-25,28] are presented in Table 6. In general, a very good agreement between computed with the PBE0/6-31G(d)+LANL2DZ method and experimental data was obtained, with the absolute error being in the range 0.03-0.09 eV. The calculated phosphorescence of blue to red colored complexes at 467 nm (2.66 eV), 570 nm (2.18 eV), 588 nm (2.11 eV), 665 nm (1.87 eV) and 693 nm (1.79 eV), were in good agreement with their corresponding experimental values at 471 nm (2.63 eV), 553 nm (2.24 eV), 576 nm (2.15 eV), 632 nm (1.96 eV) and 675 nm (1.84 eV). For all complexes, the S_0→T_1 transition showed the main H→L contribution, having ^{3}MLCT character.

Table 6. Calculated phosphorescence emissions in nm (eV) together with the corresponding experimental values of Ir(LB)$_2$(acac), Ir(LG)$_2$(acac), Ir(LY)$_2$(acac), Ir(LO)$_2$(acac) and Ir(LR)$_2$(acac).

	B3LYP/6-31G(d)+LANL2DZ	B3LYP/TZVP+def-TZVP	PBE0/6-31G(d)+LANL2DZ	PBE0/TZVP+def-TZVP	Dominant transitions and assignments	Expt.
Ir(LB)$_2$(acac)	465 (2.67)	479 (2.59)	467 (2.66)	478 (2.59)	H→L (^{3}MLCT)	471 (2.63)
Ir(LG)$_2$(acac)	581 (2.13)	597 (2.08)	570 (2.18)	583 (2.13)	H→L (^{3}MLCT)	553 (2.24)
Ir(LY)$_2$(acac)	606 (2.05)	627 (1.98)	588 (2.11)	605 (2.05)	H→L (^{3}MLCT)	576 (2.15)
Ir(LO)$_2$(acac)	677 (1.83)	695 (1.78)	665 (1.87)	679 (1.83)	H→L (^{3}MLCT)	632 (1.96)
Ir(LR)$_2$(acac)	731 (1.70)	740 (1.68)	693 (1.79)	715 (1.73)	H→L (^{3}MLCT)	675 (1.84)

4. Conclusion

Density Functional Theory (DFT) and time-dependent DFT (TD-DFT) calculations were performed to investigate in detail the blue to red colored phosphorescence of iridium complexes involved in the absorption and emission processes. Broad spectrums of color ranging from blue to red were achieved by changing of cyclometalating ligands as well as by variation of the electronic properties of the central metal by adjusting the ancillary ligands. From the TD-DFT calculations, it can be concluded that iridium complexes have a single emission

center with single excitation paths of MLCT character. We computed all the low-lying electronic states of iridium complexes as metal to ligand charge transfer (MLCT) character. Comparing of the experimental and calculated absorption spectra in wavelength regions dominated by low-lying singlet-singlet and singlet–triplet transitions, we find that B3LYP/6-31G(d)+LANL2DZ and PBE0/6-31G(d)+LANL2DZ methods perform quite well. For emission, results obtained by the PBE0/6-31G(d)+LANL2DZ method are in very good agreement with the experimental data, the absolute error being in the range 0.03-0.09 eV. Thus, we conclude that the computational analysis applied here can open the way to a theoretical and computational strategy for the design and preparation of new phosphorescent iridium compounds and the development of inorganic and organometallic photochemistry.

References

[1] Y. You, J. Soe, S. H. Kim, K. S. Kim, T. K. Ahn, D. Kim, S. Y. Park, Inorg. Chem. **47**, 1476 (2008).

[2] T. Liu, H-X. Zhang B-H. Xia, Journal of Organometallic Chemistry **693**, 947 (2008).

[3] P.J. Hay, J. Phys. Chem. A **106**, 1634 (2002).

[4] Y. H. Lee, Y. S. Kim, Thin Solid Films **515**, 5079 (2007); G.Y. Park, Y.S. Kim, Y. Ha, Current Applied Physics **7**, 390 (2007); G. Y. Park, Y. S. Kim, Y.K. Ha, Thin Solid Films **515**, 5090 (2007); C-L. Ho, W-Y. Wong, Q. Wang, D. Ma, L. Wang, Z. Lin, Adv. Func. Mater. **18**, 928 (2008).

[5] D. Di Censo, S. Fantacci, F. D. Angelis, C. Klein, N. Evans, K. Kalyanasundaram, H. J. Bolink, M. Gratzel, M. K. Nazeeruddin, Inorg. Chem. **47**, 980 (2008).

[6] A. D. Becke, J. Chem. Phys. **98**, 5648 (1993); C. Lee, W. Yang and R. G. Parr, Phys. Rev. B **37**, 785 (1988).

[7] W. Koch, M. C. Holthausen, A Chemist's Guide to Density Functional Theory, Wiley-VCH: New York, (2001).

[8] A. D. Becke, J. Phys Rev A **38**, 3098 (1988).

[9] J. Perdew, J. Phys. Rev. B **33**, 8822 (1986).

[10] M. Piacenza, I. Hyla-Kryspin and S. Grimme J Comput Chem. **28**, 2275 (2007); I. Hyla-Kryspin S. Grimme, Organometallics **23**, 5581 (2004); F. Furche, J. P. Perdew, J. Chem. Phys. **124**, 044103 (2006).

[11] R. E. Stratmann, G. E. Scuseria, M. J. Frisch, J. Chem. Phys. **109**, 8218 (1998); N. N. Matsuzawa, A. Ishitani, D. A. Dixon, T. Uda, J. Phys. Chem. A **105**, 4953 (2001); M. E. Casida, C. Jamorski, K. C. Casida, D. R. Salahub, J. Chem. Phys. **108**, 4439 (1998).

[12] A. Vlcek Jr. and S. Zalis, Coordination Chemistry Reviews **251**, 258 (2007).

[13] P. Hohenberg, W. Kohn, Phys. Rev. **136**, B864 (1964); W. Kohn and L. Sham, J. Phys. Rev. **140**, A1133 (1965); A. K. Theophilou, J. Phys. C: Solid State Phys., **12**, 5419 (**1979**); N. Hadjisavvas, A. K. Theophilou, Phys. Rev. A **30**, 2183 (1984).

[14] A. Schäfer, C. Huber, R. Ahlrichs, J. Chem. Phys. **100**, 5829 (1994).

[15] R. Ahlrichs, et al. TURBOMOLE (Vers. 6.3) Universität Karlsruhe, Karlsruhe, Germany, http://www.turbomole.com (2007).

[16] C. Adamo, V. Barone, J. Chem. Phys. **110**, 6158 (1999).

[17] D. J. Feller, Comp. Chem. **17**, 1571 (1996); K. L. Schuchardt, B. T. Didier, T. Elsethagen, L. Sun, V. Gurumoorthi, J. Chase, J. Li, T. L. Windus, J. Chem. Inf. Model. **47**, 1045 (2007).

[18] P. J. Hay, W. R. Wadt, J. Chem. Phys. **82**, 299 (1985); L. E. Roy, P.J. Hay, R. L. Martin, J. Chem. Theory Comput. **4**, 1029 (2008); A. W. Ehlers, M. Böhme, S. Dapprich, A. Gobbi, A. Höllwarth, V. Jonas, K. F. Köhler, R. Stegmann, A. Veldkamp, G. Frenking, Chem. Phys. Lett. **208**, 111 (1993).

[19] T. H. Dunning Jr, P. J. Hay, in Modern Theoretical Chemistry; H. F. Schaefer III, Ed.; Vol. 3, Plenum, New York (1977); P. J. Hay, W. R. Wadt, J. Chem. Phys. **82**, 270 (1985); W. R. Wadt, P. J. Hay, J. Chem. Phys. **82**, 284 (1985).

[20] S. Miertuš, E. Scrocco, J. Tomasi, Chem. Phys. **55**, 117 (1981); S. Miertuš, J. Tomasi, Chem. Phys. **65**, 239 (1982); J. L. Pascual-Ahuir, E. Silla I. Tuñón, J. Comp. Chem. **15**, 1127 (1994); M. Cossi, V. Barone, R. Cammi, J. Tomasi, Chem. Phys. Lett. **255**, 327 (1996); V. Barone, M. Cossi, J. Tomasi, J. Chem. Phys. **107**, 3210 (1997); E. Cancès, B. Mennucci, J. Tomasi, J. Chem. Phys. **107**, 3032 (1997); B. Mennucci and J. Tomasi, J. Chem. Phys. **106**, 5151 (1997); B. Mennucci, E. Cancès, J. Tomasi, J. Phys. Chem. B **101**, 10506 (1997); V. Barone, M. Cossi, J. Phys. Chem. A **102**, 1995 (1998); M. Cossi, V. Barone, B. Mennucci, J. Tomasi, Chem. Phys. Lett. **286**, 253 (1998); V. Barone, M. Cossi, J. Tomasi, J. Comp. Chem. **19**, 404 (1998); R. Cammi, B. Mennucci, J. Tomasi, J. Phys. Chem. A **103**, 9100 (1999); M. Cossi, V. Barone,

M. A. Robb, J. Chem. Phys. **111**, 5295 (1999);
J. Tomasi, B. Mennucci, E. Cancès, J. Mol.
Struct. (Theochem) **464**, 211 (1999); R. Cammi,
B. Mennucci, J. Tomasi, J. Phys. Chem. A
104, 5631 (2000); M. Cossi, V. Barone, J. Chem.
Phys. **112**, 2427 (2000); M. Cossi, V. Barone,
J. Chem. Phys. **115**, 4708 (2001); M. Cossi,
N. Rega, G. Scalmani, V. Barone, J. Chem. Phys.
114, 5691 (2001); M. Cossi, G. Scalmani, N. Rega
V. Barone, J. Chem. Phys. **117**, 43 (2002);
M. Cossi, N. Rega, G. Scalmani, V. Barone,
J. Comp. Chem. **24**, 669 (2003); J. Tomasi,
B. Mennucci, R. Cammi, Chem. Rev.
105, 2999 (2005).

[21] M. J. Frisch, G. W. Trucks, H. B. Schlegel,
G. E. Scuseria, M. A. Robb, J. R. Cheeseman,
G. Scalmani, V. Barone, B. Mennucci,
G. A. Petersson, H. Nakatsuji, M. Caricato, X. Li,
H. P. Hratchian, A. F. Izmaylov, J. Bloino,
G. Zheng, J. L. Sonnenberg, M. Hada, M. Ehara,
K. Toyota, R. Fukuda, J. Hasegawa, M. Ishida,
T. Nakajima, Y. Honda, O. Kitao, H. Nakai,
T. Vreven, J. A. Montgomery, Jr., J. E. Peralta,
F. Ogliaro, M. Bearpark, J. J. Heyd, E. Brothers,
K. N. Kudin, V. N. Staroverov, R. Kobayashi,
J. Normand, K. Raghavachari, A. Rendell,
J. C. Burant, S. S. Iyengar, J. Tomasi, M. Cossi,
N. Rega, J. M. Millam, M. Klene, J. E. Knox,
J. B. Cross, V. Bakken, C. Adamo, J. Jaramillo,
R. Gomperts, R. E. Stratmann, O. Yazyev,
A. J. Austin, R. Cammi, C. Pomelli,
J. W. Ochterski, R. L. Martin, K. Morokuma,
V. G. Zakrzewski, G. A. Voth, P. Salvador,
J. J. Dannenberg, S. Dapprich, A. D. Daniels,
Ö. Farkas, J. B. Foresman, J. V. Ortiz,
J. Cioslowski, D. J. Fox, Gaussian 09, (Revision
C.01), Gaussian, Inc., Wallingford CT, (2009).

[22] I. R. Laskar, S. F. Hsu, T. M Chen, Polyhedron
24, 189 (2005); S. Lamansky, P. Djurovich,
D. Murphy, F. Abdel-Razzaq, H.E. Lee,
C. Adachi, P.E. Burrows, S.R. Forrest,
M. E. Thompson, J. Am. Chem. Soc.
123, 4304 (2001); S. Lamansky, P. Djurovich,
D. Murphy, F. Abdel-Razzaq, R. Kwong,
I. Tsyba, M. Bortz, B. Mui, R. Bau,
M. E. Thompson, Inorg. Chem. **40**, 1704 (2001).

[23] G. Ge, G. Zhang, H. Guo, Y. Chuai, D. Zou,
Inorganica Chimica Acta **362**, 2231 (2009).

[24] G. Zhang, H. Guo, Y. Chuai, D. Zou, Materials
Letters **59**, 3002 (2005).

[25] Y. Ha, J. H. Seo and Y. K. Kim, Synthetic Metals
158, 548 (2008).

[26] G. L. Zhang, Z. H. Liu, H. Q. Guo, Chinese
Chemical Letters **15**, 1349 (2004).

[27] X. N. Li, Z. J. Wu, X. J. Liu and H. J. Zhang,
J. Phys. Chem. A **114**, 9300 (2010); A. Kadari,
A. Moncomble, I. Ciofini, M. Brahimi,
C. Adamo, J. Phys. Chem. A **115**, 11861 (2011);
X. Gu, T. Fei, H. Zhang, H. Xu, B. Yang, Y. Ma
X. Liu, J. Phys. Chem. A **112**, 8387 (2008);
F. D. Angelis, L. Belpassi, S. Fantacci, Journal of
Molecular Structure: THEOCHEM
914, 74 (2009); H. Gao, R. Mo, H. Zhang,
Y. Wang, Z. M. Su, Synthetic Metals
160, 1015 (2010); E. Orselli, R. Q. Albuquerque,
P. M. Fransen, R. Fröhlich, H. M. Janssen,
L. D. Cola, J. Mater. Chem. **18**, 4579 (2008);
P. T. Chou, Y. Chi, Chem. Eur. J. **13**, 380 (2007).

[28] J. Gao, H. You, J. Fang, D. Ma, L. Wang, X. Jing,
F. Wang, Synthetic Metals **155**, 168 (2005).

_____

*Corresponding author: ttugsuz@hacettepe.edu.tr